Received: 10 January 2020 | Revised: 8 April 2020 | Accepted: 25 May 2020

DOI: 10.1002/pro.3894

THE PROTEIN SOCIETY WILEY

FULL-LENGTH PAPER

Design of a surrogate Anticalin protein directed against CD98hc for preclinical studies in mice

Friedrich-Christian Deuschle | **André Schiefner** | **Corinna Brandt** | **Arne Skerra**

Lehrstuhl für Biologische Chemie, Technische Universität München, Freising, Germany

Correspondence
Arne Skerra, Lehrstuhl für Biologische Chemie, Technische Universität München, Emil-Erlenmeyer-Forum 5, 85354 Freising, Germany.
Email: skerra@tum.de

Funding information
Deutsche Forschungsgemeinschaft, Grant/Award Number: CRC 824 (A08)

Abstract

The human CD98 heavy chain (CD98hc) offers a promising biomedical target both for tumor therapy and for drug delivery to the brain. We have previously developed a cognate Anticalin protein with picomolar affinity and demonstrated its effectiveness in a xenograft animal model. Due to the lack of cross-reactivity with the murine ortholog, we now report the development and X-ray structural analysis of an Anticalin with high affinity toward CD98hc from mouse. This binding protein recognizes the same protruding epitope loop—despite distinct structure—in the membrane receptor ectodomain as the Anticalin selected against human CD98hc. Thus, this surrogate Anticalin should be useful for the preclinical assessment of CD98hc targeting in vivo and support the translational development for medical application in humans.

KEYWORDS

cancer theranostics, CD98hc, lipocalin, mouse model, protein engineering

1 | INTRODUCTION

The cluster of differentiation (CD) 98 encompasses a family of heterodimeric amino acid transporters (HATs) comprising a glycosylated type-II-transmembrane heavy chain protein (CD98hc, also referred to as 4F2hc or SLC3A2) which is covalently linked via a disulfide-bridge with one of six different light chain transporters (CD98lc, e.g., LAT-1[1] or xCT[2]). These HATs exhibit different specificities for the transport of cationic, neutral, small neutral, or negatively charged amino acids as well as thyroid hormones (T_3 and T_4) and L-3,4-dihydroxyphenylalanine.[3]

CD98hc acts as a molecular chaperon that stabilizes the CD98lc proteins and facilitates their proper membrane integration, which is essential for HAT function.[4,5] Beyond its supporting role for amino acid transport, CD98hc directly interacts with integrin β-subunits via its cytosolic N-terminal domain and the single transmembrane helix, thereby regulating adhesive cellular signaling, proliferation, survival, and migration.[6–8] Thus, CD98hc influences both activation of intracellular integrin signaling (including FAK and Akt phosphorylation[9]) as well as integrin-dependent cell-to-cell contacts (e.g., via VCAM-1 expressed on endothelial cells[10] and extracellular fibronectin matrix assembly).[11]

In accordance with its role at the crossroad of integrin function and cell metabolism, CD98hc is highly expressed in various blood cancers, including lymphoma[12] and leukemia,[10,13] and in solid tumors such as colorectal cancer,[14] non-small cell lung cancer,[13,15] triple-negative breast cancer,[16,17] and metastatic prostate cancer.[18] Thus, CD98hc has emerged as a molecular

target with potential for applications in cancer therapy and diagnosis. Indeed, investigations in several preclinical tumor models using monoclonal antibodies (mAb) or small molecule inhibitors directed toward CD98hc or CD98lc's, respectively, have demonstrated suppression of tumor growth.[10,13,19]

Apart from that, CD98hc was described as a novel transcytosis receptor expressed in the brain endothelium which can be utilized for the delivery of therapeutics to the central nervous system.[20] Efficient crossing of the blood–brain barrier (BBB) constitutes the main obstacle for the development of both biopharmaceuticals and small molecule drugs for the diagnosis and/or treatment of neurological disorders. In fact, a bispecific antibody directed against mouse CD98hc as well as to the Alzheimer amyloid precursor protein (APP) cleavage enzyme β-secretase (BACE1) showed strong accumulation in the brain after systemic dosing in a preclinical mouse model and, accordingly, a reduction in Aβ burden.[20]

We recently described the development of a high affinity Anticalin (P3D11) against human CD98hc which specifically recognizes a protruding loop structure in the membrane distal part of its extracellular domain (hCD98-hcED).[21] Of note, this part of the CD98 heterodimer is accessible regardless of the dynamic interchain motions.[22] A half-life optimized version of this Anticalin demonstrated specific binding to the cell surface protein on human cancer cell lines from different tissue origins and was successfully used, after ^{89}Zr-radiolabeling, for the in vivo positron emission tomography/computed tomography (PET/CT) imaging in a human cancer xenograft mouse model.[21]

However, this Anticalin exclusively recognizes the human membrane protein, which can be explained both by the low amino acid sequence conservation between the human and murine CD98hc orthologs at the solvent-accessible surface (~50%) as well as their differing glycosylation patterns as previously described.[23] To enable preclinical evaluation, including pharmacokinetics and safety assessment, experimental studies in rodents are of major importance. Especially for the development of BBB-penetrating agents, targeting of the murine CD98hc is crucial, due to the lack of corresponding humanized transgenic mouse strains or of reliable in vitro models to mimic the human BBB.

Here, we describe the development of a surrogate Anticalin protein directed against the murine CD98hc extracellular domain (mCD98hcED) with very similar binding characteristics compared to the Anticalin P3D11 that recognizes the human receptor, as evidenced by functional assessment as well as X-ray crystallography.

2 | RESULTS AND DISCUSSION

2.1 | Selection of a mCD98hcED-specific Anticalin with picomolar affinity

For selection via filamentous phagemid display a combinatorial library based on the human lipocalin 2 (Lcn2) scaffold carrying 20 randomized amino acid positions was used.[24] The unglycosylated mCD98hcED produced in *Escherichia coli* was immobilized to paramagnetic beads via a biotin group and employed as molecular target for the selection experiment while considering two aspects: (a) if expressed by a mammalian host cell the extensive glycosylation of mCD98hc (which accounts for ~40% of its apparent molecular mass[21]) could hamper the initial in vitro selection process of novel Anticalins via sterical hindrance and/or electrostatic repulsion from the charged oligosaccharides, as seen before in a selection campaign against prostate-specific membrane antigen[25]; (b) the differing glycosylation patterns of the human and murine CD98hc orthologs might prevent the selection of lipocalin variants against the homologous loop structure in mCD98hcED (Residues 362–411) as recognized on hCD98hcED by the previously described Anticalin P3D11.[23]

After six selection cycles, a pronounced enrichment of lipocalin variants toward the mCD98hcED was detectable (Figure S1a). From this population, the Anticalin candidate C1B12 was identified via enzyme-linked immunosorbent assay (ELISA) screening, where the corresponding clone gave rise to a strong and specific binding signal when probed with the biotinylated (unglycosylated) target protein (Figure S1b). As anticipated, most of the 20 randomized positions within the wild-type (wt)Lcn2 scaffold were mutated in the encoded amino acid sequence of the variant C1B12. Interestingly, there was no consensus in the set of amino acid exchanges if compared with the previously selected αhCD98hc Anticalin P3D11 (Figure 1a). The Anticalin candidate C1B12 was produced as a soluble protein in *E. coli* and purified to homogeneity, yielding a monomeric protein with an apparent molecular size in sodium dodecyl sulfate polyacrylamide gel electrophoresis (SDS-PAGE) similar to Lcn2, which was further confirmed by analytical size-exclusion chromatography (SEC) and electrospray ionization mass spectrometry (ESI-MS) (Figure 1b, S1(c–f), Table S1).

Real-time surface plasmon resonance (SPR) analysis resulted in an equilibrium dissociation constant (K_D) of 630 pM toward the immobilized unglycosylated mCD98-hcED, with a rather long complex half-life of 2.5 hr, hence revealing similar binding characteristics compared to the αhCD98hc Anticalin P3D11 (K_D = 150 pM)[21]

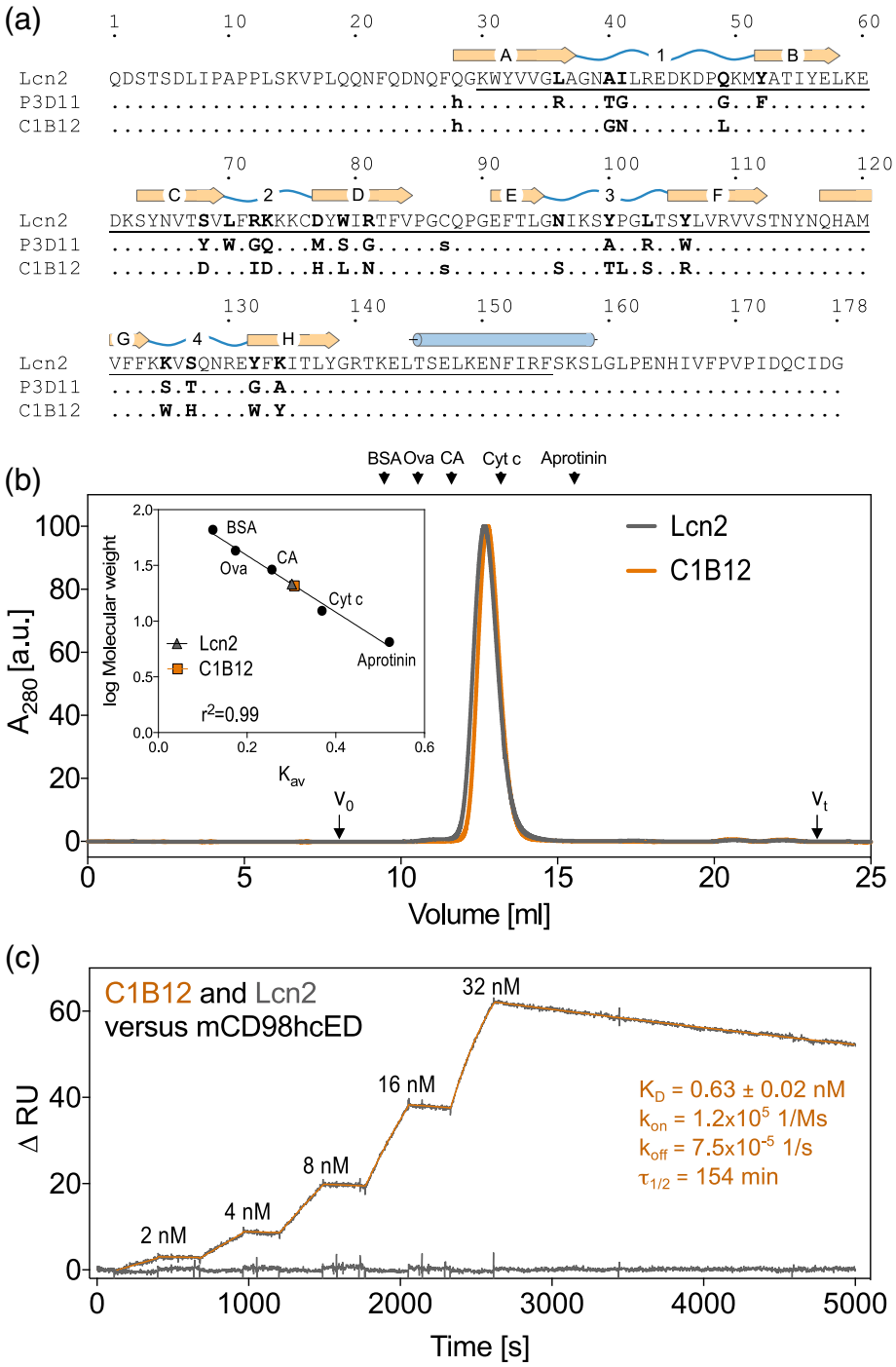

FIGURE 1 Biophysical characterization of the αmCD98hcED Anticalin C1B12. (a) Amino acid sequence alignment of the selected lipocalin variant C1B12 compared to wtLcn2 and to the αhCD98hc Anticalin P3D11. The central randomized gene cassette flanked by two *Bst*XI sites is underlined; β-strands and structurally hypervariable loops are labeled with letters A–H and numbers #1–#4, respectively. Randomized positions in the Lcn2 sequence are highlighted bold. (b) Analytical SEC profile of the mCD98hc-specific Anticalin C1B12 in comparison with recombinant wtLcn2, revealing monodispersity and a monomeric oligomerization status. From calibration runs with protein size standards a molecular weight of 20.7 kDa was deduced for C1B12 (inset). (c) Real-time SPR analysis of the Anticalin C1B12 versus mCD98hcED (produced in *E. coli*), demonstrating a picomolar dissociation constant. As expected, no binding activity of wtLcn2 toward this molecular target was detectable

(Figure 1c). Furthermore, the SPR experiments indicated that C1B12 recognizes an epitope on the unglycosylated mCD98hcED that is not fully conserved in hCD98hcED whereas, on the other hand, the epitope appeared to be shielded by N-glycosylation of a specific sequon in the murine protein (Figure S2). These findings demonstrated that both Anticalin proteins, C1B12 and P3D11, target similar epitopes at the membrane-distal side of the CD98hcED.

2.2 | X-ray structure of the C1B12·mCD98hcED complex

To gain deeper insight into the mode of epitope recognition of the murine target receptor by the Anticalin C1B12, the three-dimensional structure of its complex with mCD98hcED was elucidated by X-ray crystallography. To ensure a 1:1 stoichiometry, the C1B12·mCD98hcED complex was isolated by preparative SEC prior to crystallization

(Figure S3a–c). Crystals of mCD98hcED·C1B12 grew in space group $P2_12_12$ with two complexes per asymmetric unit. The X-ray structure of the bimolecular complex was refined to a resolution of 2.75 Å (Figure S3(d,e), Table 1).

Like its human ortholog, mCD98hcED exhibits a glycoside hydrolase fold comprising a triose-phosphate isomerase (TIM) barrel core domain (Residues 108–432) and a C-terminal β-sandwich domain (Residues 433–526) as previously described.[23] The Anticalin C1B12 binds to the membrane-distal part of mCD98hcED via its four engineered loops, #1–#4 (Figure 2), as anticipated. The contact interface involves a total buried surface area (BSA) of 1,363 Å^2, with 1,340 Å^2 on the side of the lipocalin and 1,386 Å^2 on the one of mCD98hcED, including 15 hydrogen bonds and 3 salt bridges (Tables S2 and S3).

mCD98hcED is recognized by the Anticalin via three epitope regions, here referred to as L2, L3, and L4. The majority of the contacts are contributed by L2 (Residues 362–411), that is, the loop downstream of the eighth β-strand of the TIM barrel. L2 reaches deeply into the ligand pocket of the lipocalin variant C1B12 and contributes 76% to the interface. Upon binding to C1B12, L2 undergoes a significant conformational change (Table S3) compared with the uncomplexed mCD98hcED.[23] The largest structural difference is observed at its tightly buried tip (Residues 392–395, Ile-Pro-Arg-Pro; cf. Figure S4), with an average Cα root mean square deviation of 12 Å versus the uncomplexed L2 (after superposition of the TIM barrel core). Notably, this conformational change is accompanied by concerted *cis*/*trans* and *trans*/*cis* isomerizations of the peptide bonds N-terminal to residues Pro393 and Pro395 in L2, respectively. Further contacts between the Anticalin and mCD98hcED are mediated by L3 (Residues 340–345), including parts of both the loop and the α-helix that follow the seventh β-strand of the TIM barrel, as well as the discontinuous stretch of L4 (Residues 493–499 and 513–515) in the C-terminal β-sandwich domain (Figure 2b, Table S3).

TABLE 1 X-ray data collection and refinement statistics

Data collection	
Space group	$P2_12_12$
Unit cell parameters	$a = 105.04$ Å, $b = 107.74$ Å, $c = 133.87$ Å, $\alpha = \beta = \gamma = 90°$
Wavelength [Å]	0.9184
Resolution [Å]	35.0–2.75 (2.85–2.75)[a]
Completeness [%]	99.1 (96.6)
Unique reflections	39,856 (3,894)
Multiplicity	13.2 (11.7)
Mean I/σ(I)	15.4 (2.5)
R_{meas} [%]	20.5 (112.8)
Wilson *B*-factor [Å]	42.7
Refinement	
Resolution [Å]	34.71–2.75 (2.82–2.75)
Reflections (working)	37,895 (2,701)
Reflections (test)[b]	1,961 (116)
R_{cryst} [%]	22.0 (34.2)
R_{free} [%]	27.0 (39.6)
Protein molecules per asymmetric unit	4
Number of atoms: protein/solvent[c]	9,424/206
B-values of atoms: protein/solvent [Å^2]	47.6/39.0
Ramachandran plot[d]: favored/outliers [%]	96.1/0.2
RMSD bonds [Å]/angles [°]	0.002/1.182

Abbreviation: RMSD, root mean square deviation.
[a]Values in parentheses refer to the highest resolution shell.
[b]The test set corresponds to 5% of all reflections.
[c]Solvent refers to ions, water, buffer, or cryoprotectant molecules.
[d]Ramachandran statistics were calculated with MolProbity.[26]

2.3 | Structural comparison of the surrogate Anticalin pair

Both Anticalins, C1B12 and P3D11, recognize their CD98hc targets with affinities in the pM range while exhibiting comparable BSA values and the same number of hydrogen bonds and salt bridges in the three-dimensional structures of the corresponding complexes (Table S2). Superposition of C1B12·mCD98hcED with P3D11·hCD98hcED via the homologous murine/human CD98hc target molecules and subsequent analysis of the binding mode of C1B12 in relation to P3D11 revealed a 153° rotation around the lipocalin β-barrel axis and a 14 Å shift toward the C-terminus of the CD98hcED (Figure 2). As result, P3D11 predominantly binds the epitope regions L1 and L2 of hCD98hcED,[21] whereas C1B12 interacts with L2, L3, and L4 of mCD98hcED, as explained above (Figures 2 and S5).

Nevertheless, in both cases the protruding L2 loop constitutes the major epitope and contributes ~75% of all contacts, even though this structural element is approached by the two Anticalins from different directions. The engineered lipocalin C1B12 predominantly recognizes L2 via its loop #4, the β-barrel core and loop #1, whereas loop #1, the β-barrel core and loop #2 dominate the interactions of P3D11 with L2 (Figure 2,

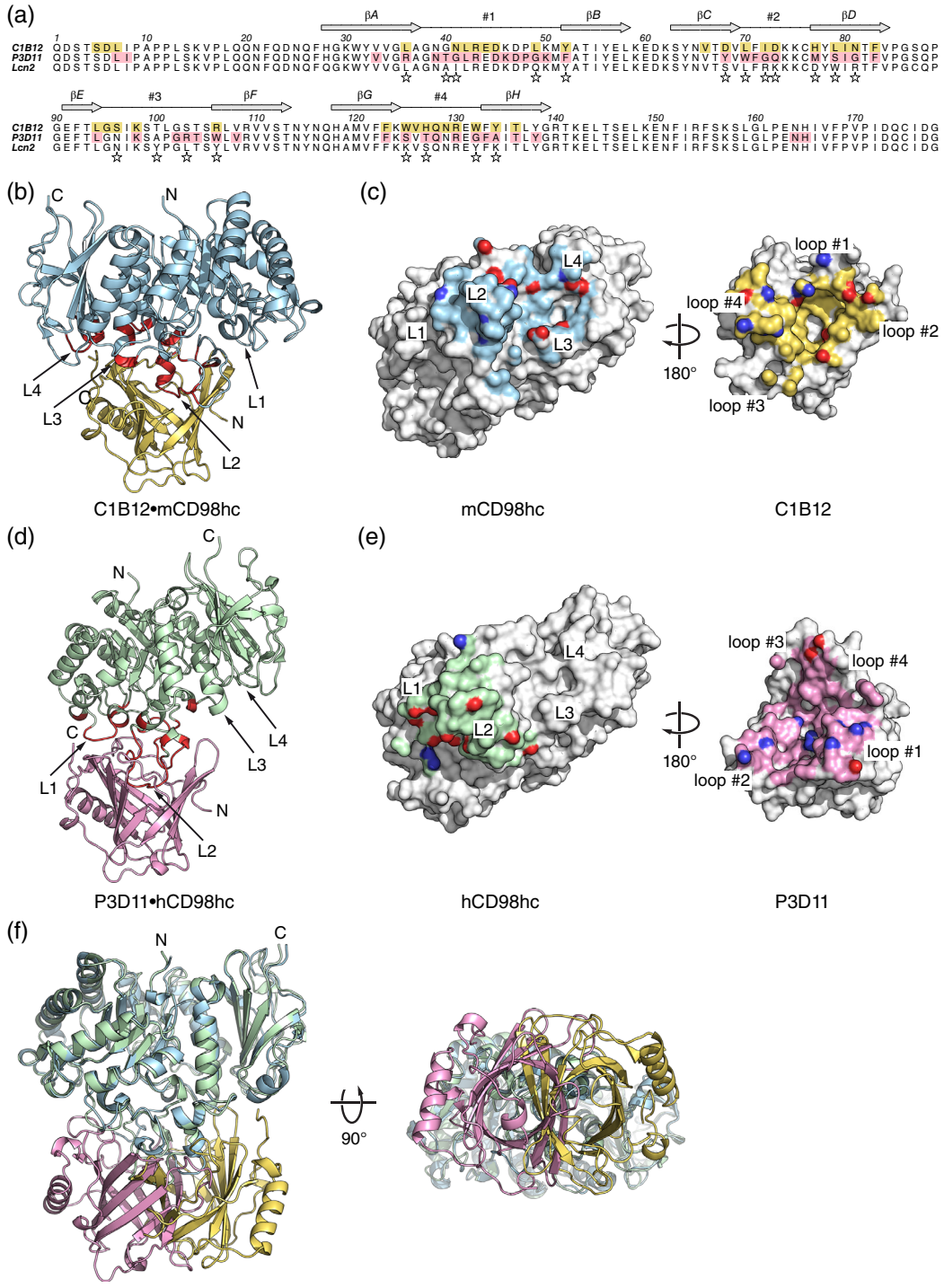

FIGURE 2 Structural comparison of the Anticalin complexes with the murine and human CD98hc target proteins. (a) Contact analysis of the two Anticalins C1B12 and P3D11. Residues that interact with mCD98hc and hCD98hc, respectively, are highlighted in the amino acid sequence with the same color (yellow or pink, respectively) as used for each Anticalin in the crystal structures shown below. Stars denote the randomized positions in the wtLcn2 sequence. (b, d) Crystal structure of C1B12 (yellow) in complex with mCD98hc (light blue) (Table 1) in comparison with P3D11 (pink) in complex with hCD98hc (light green) (PDB ID: 6S8V). The two Anticalins are shown in the same orientation and the residues in both CD98hc epitopes are highlighted red (Table S3). (c, e) View of the buried molecular surfaces for C1B12·mCD98hc and P3D11·hCD98hc, respectively, after separation of the complex partners. The contacting residues are colored like the individual molecules in (b) and (d), whereas noncontacting residues are shown in light gray. Hydrogen bond as well as salt bridge donor/acceptors are highlighted blue and red, respectively. (f) Superposition of the murine and human CD98hcED target proteins reveals differences in the mode of recognition by their cognate Anticalins, C1B12 and P3D11, as evident from their relative rotation by almost 180° and the mutual shift

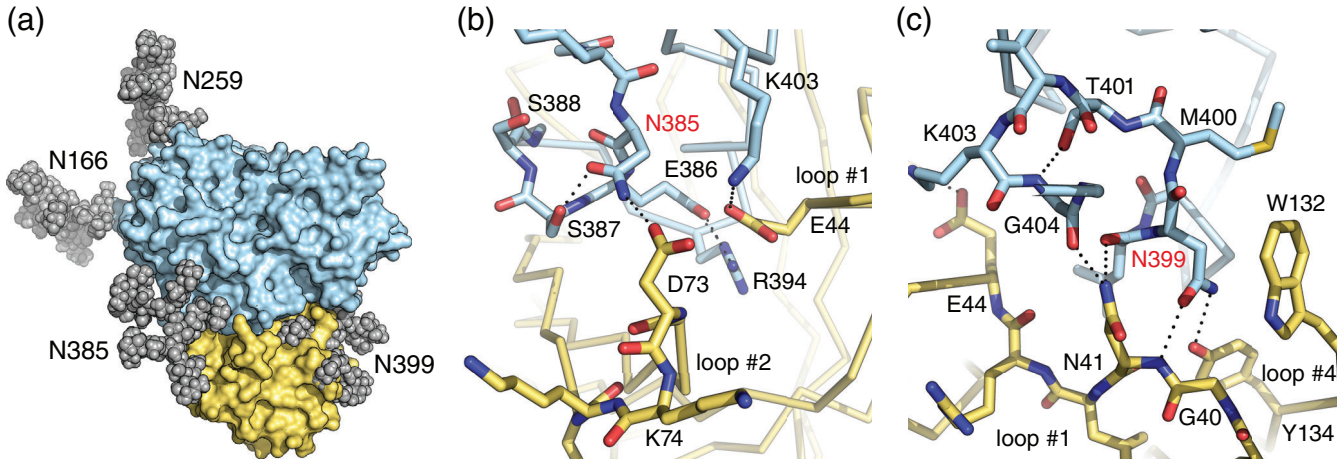

FIGURE 3 Effect of N-glycosylation on the interaction between mCD98hc and C1B12. (a) mCD98hcED with modeled glycan structures and the bound Anticalin C1B12 in the crystallized complex,[23] illustrating potential interference of the oligosaccharides attached to Asn385 and, in particular, Asn399. (b, c) Close-up views of contacts between the Asn385 (b) and Asn399 (c) side chains in the unglycosylated mCD98hcED and the bound Anticalin C1B12

Table S2). Interestingly, in both Anticalins the contribution of loop #3 to the interface with the target is marginal, but at the same time this loop shows the largest structural deviation from wtLcn2 (Figure S4, Table S2). This suggests that in both Anticalins loop #3 has to bend away from the calyx axis to create space for tight complex formation with CD98hc.

Comparison of the electrostatics revealed a slightly less acidic membrane-distal surface for mCD98hcED than for hCD98hcED, which is consistent with their differing theoretical p*I* values of 5.9 and 5.2, respectively.[23] In particular, L2 shows a different Coulomb potential in the context of the two Anticalins, which is slightly positive for mCD98hcED but slightly negative for hCD98hcED (Figure S5). These surface charges are complemented by the negatively or positively charged electrostatic potential of the ligand-binding sites in the lipocalin variants C1B12 and P3D11, respectively. Still, both Anticalins also match the slightly hydrophobic character of L2 in the two CD98hcED target molecules (Figure S5).

2.4 | Role of N-glycosylation for the molecular recognition of mCD98hcED as a protein target

In vivo, the L2 epitope region of mCD98hc is N-glycosylated at two positions, Asn385 and Asn399, of which Asn385 is unique to the murine ortholog.[23,27] Although this Asn residue in the target protein forms a hydrogen bond with loop #2 of the Anticalin C1B12 in the crystal structure of the complex, its location at the fringe of the interface suggests that this N-glycosylation should have minor influence on the binding interaction (Figure 3). On the other hand, a free Asn399 side chain is essential for the tight interaction with C1B12 as it forms hydrogen bonds with Asn41 and Tyr134 as well as a stacking interaction with Trp132 of the Anticalin (Figure 3c). Obviously, N-glycosylation at this site should abolish binding between C1B12 and the mCD98hcED, which is consistent with the findings from our SPR experiments (cf. Figure S2, Table S4).

Consequently, to utilize C1B12 as a viable surrogate Anticalin for targeting mCD98hc in vivo, N-glycosylation ideally at both Asn residues should be prevented in order to avoid disruption of the epitope. In the case of Asn399 this may be simply achieved by altering the third position of the NMT glycosylation sequon, Thr401, to Ala. Due to its smaller side chain, Ala causes only minimal structural perturbation within the mCD98hc epitope, just accompanied by loss of a hydrogen bond with the main chain nitrogen of Gly404 (Figure 3c). In the light of its proximity to the C1B12 epitope, as explained above, glycosylation of Asn385 might interfere with binding of the Anticalin, too. However, this can be resolved via substitution by Asp, the equivalent residue in the human ortholog (UniProt ID P08195-2: Asp392).[23] Such a double mutant of mCD98hc may be incorporated into a transgenic mouse model, for example, by replacing exon no. 8 by a mutated version with the help of CRISPR/Cas9 technology.[28]

In order to validate this concept from a protein functional perspective, the corresponding mCD98hcED (N385D/T401A) mutant was produced both as a soluble protein in *E. coli* BL21 and (partially) glycosylated—at Asn166 and Asn259, but not at Positions 385 and 399—in

human embryonic kidney (HEK) cells. Both proteins were purified to homogeneity, yielding monodisperse and monomeric preparations (Figure S6). The apparent molecular size in SEC and SDS-PAGE of the unglycosylated mCD98hcED(N385D/T401A) was similar to the unglycosylated wild-type protein. In contrast, glycosylation of the mCD98hcED(N385D/T401A) led to an increase in the apparent size compared to both unglycosylated proteins, as expected, but not to the same extent as for the fully glycosylated wild-type mCD98hcED produced in HEK cells. Notably, the double substitution just marginally affected binding activity by the Anticalin C1B12, irrespective of the remaining glycosylation at Asn166 and Asn259 (Table S4).

Thus, the Anticalin C1B12 would be suitable for in vivo targeting of the mutant mCD98hc(N385D/T401A) in a transgenic mouse model. While the two proposed mutations in mCD98hc abolish N-glycosylation within the epitope region, the lack of oligosaccharides at both positions, Asn385 and Asn399, does not affect protein folding or stability of mCD98hcED. Furthermore, even though glycosylation of CD98hc plays a role for interaction with galectin-3 in vivo,[29] the recognition by this carbohydrate-binding protein should be maintained with the remaining two glycosylation sites.

3 | CONCLUSIONS AND OUTLOOK

Targeting of CD98hc in vivo constitutes a promising approach for several biomedical applications. However, due to its high cross-species variability, both concerning the amino acid surface and glycosylation pattern, it is difficult to raise antibodies or other binding proteins with suitable species cross-reactivity. At the same time, substitution of the entire CD98hcED in a transgenic mouse by the human counterpart could likely provoke functional impairment due to the distinct protein properties. To enable a surrogate strategy for preclinical research, we have developed a high affinity Anticalin toward mCD98hc with very similar affinity and mode of epitope recognition as our previously developed αhCD98hc Anticalin, P3D11.[21] The preclinical application of the C1B12 Anticalin in a rodent animal model in vivo would require the generation of a transgenic mouse that carries just two point mutations in mCD98hc. Assuming availability of such a mouse model, our surrogate αmCD98hc/αhCD98hc Anticalin pair bears potential for pharmacokinetic and -dynamic studies to assess the in vivo targeting of CD98hc for diagnostic and therapeutic applications in oncology as well as diseases of the central nervous system.

4 | MATERIALS AND METHODS

4.1 | Phage display selection and preparation of mCD98hcED-specific lipocalin variants

Production of the biotinylated recombinant mCD98hcED both in *E. coli* BL21 and in MEXi-293E cells was performed as previously described.[21] To generate the mCD98hcED double mutant N385D/T401A, amino acid substitutions were introduced using the QuikChange site-directed mutagenesis technique (Agilent, Santa Clara, CA) with appropriate oligodeoxynucleotide pairs (Eurofins, Ebersberg, Germany) carrying the mutated codons. To be used as a target for phage display selection, unglycosylated mCD98hcED was immobilized on paramagnetic beads (Sigma–Aldrich, Munich, Germany and Thermo Fisher Scientific, Waltham, MA, respectively) coated with NeutrAvidin (Cycles 1, 3, and 5) or streptavidin (Cycles 2, 4, and 6) in an alternating fashion. The functionalized beads were incubated with a phagemid library of the randomized Lcn2 scaffold[24] (starting titer 1×10^{12}) and, after extensive washing with phosphate-buffered saline (PBS; 4 mM KH_2PO_4, 160 mM Na_2HPO_4, 115 mM NaCl pH 7.4), bound phagemids were eluted using 4 M urea. After six consecutive phagemid panning cycles, pooled phasmid DNA from the enriched library (i.e., the amplified phagemids eluted in the last step) was prepared and subcloned on pNGAL98 in order to perform ELISA screening using microcultures expressing the soluble lipocalin variants equipped with a C-terminal *Strep*-tag II.[30]

Therefore, the periplasmic extract was prepared in a microtiter plate and transferred to a 96-well MaxiSorp plate (Thermo Fisher Scientific) which had been coated with 10 μg/ml *Strep*MAB-Immo (IBA, Göttingen, Germany). After 1 hr incubation and washing steps, the selectively adsorbed lipocalin variants were incubated with the biotinylated mCD98hcED or, as negative control, biotinylated ovalbumin or PBS, followed by detection of the bound biotinylated target protein with ExtrAvidin/alkaline phosphatase (AP) conjugate (Sigma–Aldrich). Signals were developed with 0.5 mg/ml p-nitrophenyl phosphate in AP buffer (0.1 M NaCl, 5 mM $MgCl_2$, 0.1 M Tris/HCl pH 8.8), and the absorbance was measured at 405 nm in a Synergy 2 photometer (BioTek Instruments, Winooski, VT). For clones expressing lipocalin variants that revealed a significant binding signal toward mCD98hcED, the plasmid was isolated and the expression cassette was subjected to DNA sequencing.

Then, the corresponding soluble lipocalin variant was produced with a C-terminal His_6-tag using the plasmid pNGAL118 at preparative scale in a 2 L culture of *E. coli* JM83 in 2xYT medium according to a published

procedure.[24] After periplasmic protein extraction, the recombinant protein was purified by immobilized metal ion affinity chromatography using a Ni(II)-charged HisTrap HP column (GE Healthcare, Munich, Germany) and further subjected to SEC in PBS on a 24 ml Superdex 75 10/300 GL column (GE Healthcare). Protein purity and integrity were assessed using SDS-PAGE and ESI-MS, respectively, as previously described.[21]

4.2 | Biomolecular interaction analysis

Real-time SPR spectroscopy were performed as previously described.[21] Briefly, the biotinylated murine CD98hcED, or its double mutant N385D/T401A, produced in *E. coli* or in MEXi-293E cells (5 μg/ml protein solution in 10 mM HEPES/NaOH pH 7.5, 150 mM NaCl and 0.05% [vol/vol] Tween) was immobilized (ΔRU ≈ 225) to a streptavidin-coated sensorchip using the Biotin CAPture kit (GE Healthcare). Single cycle kinetic experiments were performed on a Biacore 2000 instrument (GE Healthcare) using five consecutive injections from a 1:2 dilution series of the purified lipocalin variant at a flow rate of 25 μl/min with 288 s contact time, followed by a long 3,500 s dissociation time for the highest concentration. Rate constants of association and dissociation were calculated from reference-corrected sensorgrams by fitting to a 1:1 Langmuir binding model using BIAevaluation software. The equilibrium dissociation constant (K_D) was calculated as the quotient k_{off}/k_{on}. Furthermore, to investigate binding toward the fully glycosylated mCD98hcED (mCD98hcEDg; produced in MEXi-293E cells), or to assess cross-reactivity with hCD98hcED (produced in *E. coli*), only a single concentration (1 μM) of the lipocalin variant C1B12 was injected using the same conditions as described above.

4.3 | Protein crystallization, structure determination and analysis

For protein crystallization, unglycosylated mCD98hcED was produced with an N-terminal *Strep*-tag II in *E. coli* BL21 as previously described.[23] After incubation with the Anticalin C1B12 at 1:1 molar ratio for 2 hr at 4°C, the C1B12·mCD98hcED complex was isolated via SEC on a Superdex 200 10/300 GL column (GE Healthcare) and eluted in crystallization buffer (10 mM Hepes/NaOH pH 7.5, 0.1 M NaCl, 0.02% [wt/vol] NaN_3). The complex was concentrated to ~30 mg/ml using a 30 kDa cut-off Amicon ultrafiltration unit (Merck Millipore, Burlington, MA) and subjected to crystallization by vapor diffusion at 20°C using an in-house precipitant screen. Diffraction quality crystals of plate-like morphology were obtained in hanging drops by mixing 0.5 μl C1B12·mCD98hcED with 0.5 μl reservoir solution containing 12% (wt/vol) polyethylene glycol 8,000 and 0.2 M Li_2SO_4. The crystals were transferred into cryo-protectant solution consisting of reservoir solution supplemented with 25% (vol/vol) ethylene glycol and flash frozen in liquid nitrogen. X-ray diffraction data were collected at the Helmholtz-Zentrum Berlin, Germany, BESSY beamline 14.2,[31] and reduced with the XDS package[32] (Table 1). The crystal structure was solved by molecular replacement with Phaser[33] using coordinate sets of the mCD98hcED (PDB ID: 6I9Q[23]) and the Anticalin P3D11 (PDB entry: 6S8V[21]) as separate search models. Manual rebuilding and refinement were performed with Coot[34] and Refmac5,[35] respectively (Table 1). Electrostatic surface potentials were calculated with APBS,[36] molecular packing analyses were performed with PISA[37] and molecular graphics were prepared with PyMOL (Schödinger, Cambridge, MA). The asymmetric unit of space group $P2_12_12$ contained two highly similar C1B12·mCD98hcED complexes, of which the complex comprising the chain pair A and B was used for further analysis due to its overall lower B-factors. Complex N-glycans were modeled on mCD98hcED as previously described.[23] Atomic coordinates and structure factors for the C1B12·mCD98hcED complex have been deposited in the PDB (www.rcsb.org/pdb) under the accession code 6SUA.

ACKNOWLEDGEMENTS

The authors wish to thank the Helmholtz-Zentrum Berlin, Germany, for allocation of synchrotron radiation beamtime and travel support and Dr. Christian Feiler for assistance at BESSY beamline 14.2. This work was financially supported by the German Research Foundation (DFG) in frame of the Collaborative Research Centre 824 (project A08). Anticalin® is a registered trademark of Pieris Pharmaceuticals GmbH.

AUTHOR CONTRIBUTIONS

Friedrich-Christian Deuschle: Conceptualization; investigation; methodology; validation; visualization; writing-original draft; writing-review and editing. **André Schiefner:** Conceptualization; investigation; methodology; validation; visualization; writing-original draft; writing-review and editing. **Corinna Brandt:** Investigation; validation; visualization; writing-original draft. **Arne Skerra:** Conceptualization; funding acquisition; project administration; resources; supervision; validation; visualization; writing-original draft; writing-review and editing.

CONFLICT OF INTEREST

A. Skerra is founder and shareholder of Pieris Pharmaceuticals, Inc.

ORCID

Friedrich-Christian Deuschle https://orcid.org/0000-0001-5603-3109
André Schiefner https://orcid.org/0000-0001-5215-4122
Corinna Brandt https://orcid.org/0000-0003-4443-6095
Arne Skerra https://orcid.org/0000-0002-5717-498X

REFERENCES

1. Kanai Y, Segawa H, Miyamoto K, Uchino H, Takeda E, Endou H. Expression cloning and characterization of a transporter for large neutral amino acids activated by the heavy chain of 4F2 antigen (CD98). J Biol Chem. 1998;273:23629–23632.
2. Sato H, Tamba M, Ishii T, Bannai S. Cloning and expression of a plasma membrane cystine/glutamate exchange transporter composed of two distinct proteins. J Biol Chem. 1999;274:11455–11458.
3. Fotiadis D, Kanai Y, Palacin M. The SLC3 and SLC7 families of amino acid transporters. Mol Aspects Med. 2013;34:139–158.
4. Nakamura E, Sato M, Yang H, et al. 4F2 (CD98) heavy chain is associated covalently with an amino acid transporter and controls intracellular trafficking and membrane topology of 4F2 heterodimer. J Biol Chem. 1999;274:3009–3016.
5. Yan R, Zhao X, Lei J, Zhou Q. Structure of the human LAT1-4F2hc heteromeric amino acid transporter complex. Nature. 2019;568:127–130.
6. Cantor JM, Ginsberg MH, Rose DM. Integrin-associated proteins as potential therapeutic targets. Immunol Rev. 2008;223:236–251.
7. Fenczik CA, Zent R, Dellos M, et al. Distinct domains of CD98hc regulate integrins and amino acid transport. J Biol Chem. 2001;276:8746–8752.
8. Feral CC, Nishiya N, Fenczik CA, Stuhlmann H, Slepak M, Ginsberg MH. CD98hc (SLC3A2) mediates integrin signaling. Proc Natl Acad Sci U S A. 2005;102:355–360.
9. Cai S, Bulus N, Fonseca-Siesser PM, et al. CD98 modulates integrin β1 function in polarized epithelial cells. J Cell Sci. 2005;118:889–899.
10. Bajaj J, Konuma T, Lytle NK, et al. CD98-mediated adhesive signaling enables the establishment and propagation of acute myelogenous leukemia. Cancer Cell. 2016;30:792–805.
11. Feral CC, Zijlstra A, Tkachenko E, et al. CD98hc (SLC3A2) participates in fibronectin matrix assembly by mediating integrin signaling. J Cell Biol. 2007;178:701–711.
12. Salter DM, Krajewski AS, Sheehan T, Turner G, Cuthbert RJ, McLean A. Prognostic significance of activation and differentiation antigen expression in B-cell non-Hodgkin's lymphoma. J Pathol. 1989;159:211–220.
13. Hayes GM, Chinn L, Cantor JM, et al. Antitumor activity of an anti-CD98 antibody. Int J Cancer. 2015;137:710–720.
14. Ye Y, Wang M, Wang B, Yang X-M, Chen Z-N. CD98, a potential diagnostic cancer-related biomarker, and its prognostic impact in colorectal cancer patients. Int J Clin Exp Pathol. 2017;10:5418–5429.
15. Kaira K, Oriuchi N, Imai H, et al. CD98 expression is associated with poor prognosis in resected non-small-cell lung cancer with lymph node metastases. Ann Surg Oncol. 2009;16:3473–3481.
16. El Ansari R, Craze ML, Diez-Rodriguez M, et al. The multifunctional solute carrier 3A2 (SLC3A2) confers a poor prognosis in the highly proliferative breast cancer subtypes. Brit J Cancer. 2018;118:1115–1122.
17. Furuya M, Horiguchi J, Nakajima H, Kanai Y, Oyama T. Correlation of L-type amino acid transporter 1 and CD98 expression with triple negative breast cancer prognosis. Cancer Sci. 2012;103:382–389.
18. Wang Q, Tiffen J, Bailey CG, et al. Targeting amino acid transport in metastatic castration-resistant prostate cancer: Effects on cell cycle, cell growth and tumor development. J Natl Cancer Inst. 2013;105:1463–1473.
19. Wang Q, Holst J. L-type amino acid transport and cancer: Targeting the mTORC1 pathway to inhibit neoplasia. Am J Cancer Res. 2015;5:1281–1294.
20. Zuchero YJ, Chen X, Bien-Ly N, et al. Discovery of novel blood–brain barrier targets to enhance brain uptake of therapeutic antibodies. Neuron. 2016;89:70–82.
21. Deuschle FC, Morath V, Schiefner A, et al. Development of a high affinity Anticalin® directed against human CD98hc for theranostic applications. Theranostics. 2020;10:2172–2187.
22. Chiduza GN, Johnson RM, Wright GSA, Antonyuk SV, Muench SP, Hasnain SS. LAT1 (SLC7A5) and CD98hc (SLC3A2) complex dynamics revealed by single-particle cryo-EM. Acta Crystallogr. 2019;D75:660–669.
23. Deuschle FC, Schiefner A, Skerra A. Structural differences between the ectodomains of murine and human CD98hc. Proteins. 2019;87:693–698.
24. Gebauer M, Schiefner A, Matschiner G, Skerra A. Combinatorial design of an Anticalin directed against the extra-domain B for the specific targeting of oncofetal fibronectin. J Mol Biol. 2013;425:780–802.
25. Barinka C, Ptacek J, Richter A, Novakova Z, Morath V, Skerra A. Selection and characterization of Anticalins targeting human prostate-specific membrane antigen (PSMA). Protein Eng Des Sel. 2016;29:105–115.
26. Davis IW, Leaver-Fay A, Chen VB, et al. MolProbity: All-atom contacts and structure validation for proteins and nucleic acids. Nucleic Acids Res. 2007;35:W375–W383.
27. Wollscheid B, Bausch-Fluck D, Henderson C, et al. Mass-spectrometric identification and relative quantification of N-linked cell surface glycoproteins. Nat Biotechnol. 2009;27:378–386.
28. Wright AV, Nunez JK, Doudna JA. Biology and applications of CRISPR systems: Harnessing nature's toolbox for genome engineering. Cell. 2016;164:29–44.
29. Dalton P, Christian H, Redman C, Sargent I, Boyd C. Membrane trafficking of CD98 and its ligand galectin 3 in BeWo cells—Implication for placental cell fusion. FEBS J. 2007;274:2715–2727.
30. Gebauer M, Skerra A. Anticalins: small engineered binding proteins based on the lipocalin scaffold. Methods Enzymol. 2012;503:157–188.
31. Mueller U, Darowski N, Fuchs MR, et al. Facilities for macromolecular crystallography at the Helmholtz-Zentrum Berlin. J Synchrotron Radiat. 2012;19:442–449.

32. Kabsch W. XDS. Acta Crystallogr. 2010;D66:125–132.
33. McCoy AJ, Grosse-Kunstleve RW, Adams PD, Winn MD, Storoni LC, Read RJ. Phaser crystallographic software. J Appl Cryst. 2007;40:658–674.
34. Emsley P, Lohkamp B, Scott WG, Cowtan K. Features and development of Coot. Acta Cryst. 2010;D66:486–501.
35. Murshudov GN, Skubak P, Lebedev AA, et al. REFMAC5 for the refinement of macromolecular crystal structures. Acta Cryst. 2011;D67:355–367.
36. Baker NA, Sept D, Joseph S, Holst MJ, McCammon JA. Electrostatics of nanosystems: Application to microtubules and the ribosome. Proc Natl Acad Sci U S A. 2001;98:10037–10041.
37. Krissinel E, Henrick K. Inference of macromolecular assemblies from crystalline state. J Mol Biol. 2007;372:774–797.

SUPPORTING INFORMATION

Additional supporting information may be found online in the Supporting Information section at the end of this article.

How to cite this article: Deuschle F-C, Schiefner A, Brandt C, Skerra A. Design of a surrogate Anticalin protein directed against CD98hc for preclinical studies in mice. *Protein Science*. 2020;29:1774–1783. https://doi.org/10.1002/pro.3894